Effect of Magnesium Ions on the Conformation of Two Highly Purified Yeast Alanine Transfer Ribonucleic Acids*

Robert H. Reeves,† Charles R. Cantor,‡ and Robert W. Chambers§

ABSTRACT: The effect of magnesium ions on the conformation of two highly purified yeast alanine tRNAs has been studied by optical methods. The results indicate that both have base paired conformations in the absence of Mg^{2+}. When Mg^{2+} is added, both tRNAs undergo similar conformational changes involving a net increase in base pairs (40%) and a reduction of molecular volume. We interpret this change as a completion of secondary structure, either by rearrangement of existing base pairs or formation of new ones, followed by folding of the tRNA into a tertiary structure containing still more base pairs. In spite of these similarities, $tRNA^{Ala}_{Iab}$ and $tRNA^{Ala}_{II}$ can be distinguished easily by their melting curves, their ultraviolet absorption spectra, or their circular dichroism spectra. Their denaturation behavior is also different: the alanine acceptor activity of $tRNA^{Ala}_{Iab}$ is almost completely destroyed when Mg^{2+} is added to a magnesium-free solution of the tRNA at 0°, but no loss of activity occurs when $tRNA^{Ala}_{II}$ is treated under similar conditions. Denatured $tRNA^{Ala}_{Iab}$ regains 80% of its activity by raising the temperature to 37° in the presence of Mg^{2+}. We interpret this denaturation behavior as follows: in order for an active conformation to form when Mg^{2+} is added to the tRNA solution, the cloverleaf secondary structure must form prior to the folding process that establishes a tertiary structure. When the folding process occurs with some other secondary structure, then a denatured molecule is produced. Renaturation can be effected by heating the solution, thus disrupting the tertiary structure and allowing rearrangement of the secondary structure to the cloverleaf followed by refolding.

As part of our research on structure–action relationships in tRNA, we have prepared two highly purified yeast alanine tRNAs which differ from each other in 13–18 places[1] including the "wobble base" of the anticodon (Reeves *et al.*, 1968; Imura *et al.*, 1969a). Each of these preparations is free of denatured material as judged by their ability to accept alanine. One of them, $tRNA^{Ala}_{II}$, is also chemically homogeneous as judged by its oligonucleotide pattern after digestion with RNase T-1 (Reeves *et al.*, 1968). The other, $tRNA^{Ala}_{Iab}$, is still a mixture of two species which differ by a single base (Holley *et al.*, 1965).[2]

In order to compare the properties of these isoaccepting tRNAs, we have examined their melting curves, their ultraviolet absorption spectra, their circular dichroism spectra, their hydrodynamic behavior (gel filtration and ultracentrifugation), and their denaturation in the presence and absence of magnesium ions.[3]

The results indicate that $tRNA^{Ala}_{Iab}$ and $tRNA^{Ala}_{II}$ have grossly similar ordered structures. Both seem to exist in partially base paired (66% of the maximum) conformations in the absence of magnesium ions. When Mg^{2+} is added, both tRNAs undergo similar conformational changes involving a net increase in base pairs (33%) and a reduction of molecular volume. In spite of these similarities, $tRNA^{Ala}_{Iab}$ and $tRNA^{Ala}_{II}$ can be easily distinguished by their ultraviolet or circular dichroism spectra, their T_m values, or their denaturation behavior. This indicates that important differences exist in their ordered structures that are reflected in both their chemical and biological properties.

Results

The Mg^{2+} Effect. It has been known for some time that magnesium ions exert a profound influence on the conformation of tRNA in solution. Studies of the ultraviolet absorption spectra of unfractionated tRNAs showed that a substantial increase in ordered structure occurs when

* From the Department of Biochemistry, New York University School of Medicine, New York, New York (R. H. R. and R. W. C.), and the Departments of Chemistry and Biological Sciences, Columbia University, New York, New York (C. R. C.). *Received January 26, 1970.* This work was supported by grants from the U. S. Public Health Service (5 RO1 GM 07262-10 and 5 RO1 GM 14825-03) and the American Cancer Society (P-476). Previous paper in this series, Imura *et al.* (1969c).

† U. S. P. H. S. training frant fellow (5T1 GM 1234). Present address, Department of Molecular Biology, University of California, Berkeley.

‡ Alfred P. Sloan fellow.

§ Recipient of a Career Research Scientist Award from the Health Research Council of the City of New York (I-200); to whom to address inquiries.

[1] The ambiguity is due to uncertainties in the $tRNA^{Ala}_{II}$ sequence at the present stage of our structural analysis.

[2] The ab in the subscript Iab refers to oligonucleotides eluting as peaks 13a and 13b from DEAE-cellulose chromatography of an RNase T-1 digest of $tRNA^{Ala}_{Iab}$ (Holley *et al.*, 1965). We have suggested, however (Reeves *et al.*), that roman numerals be used to designate different gene products (*i.e.*, tRNAs differing in a major base) and lower case letters be used to differentiate tRNAs that differ only in the modification of one or more major bases. Thus, $tRNA^{Ala}_{Is}$ contains a dihydrouridine residue at position 48 instead of the uridine residue found in $tRNA^{Ala}_{Ib}$.

[3] Throughout this paper we will refer to tRNA solutions "in the absence of Mg^{2+}." We mean, in the absence of *added* Mg^{2+}, where $[Mg^{2+}] < 10^{-6}$ M. If not specified more exactly, in the presence of Mg^{2+}" means added $[Mg^{2+}] > 10^{-3}$ M. This concentration range (10^{-6}–10^{-3} M) corresponds to the disorder–order transition shown in Figure 1. The only other cation present in these experiments was the conjugate acid of tris(hydroxymethyl)aminomethane.

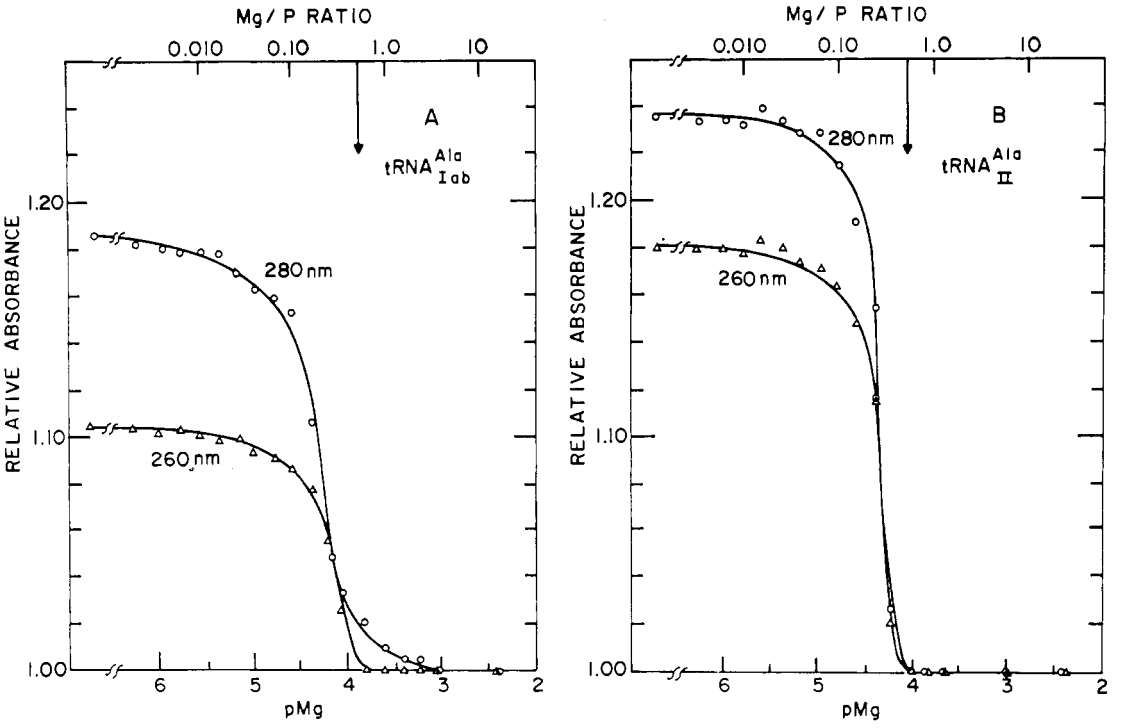

FIGURE 1: Spectrophotometric titration of $tRNA^{Ala}_{Iab}$ and $tRNA^{Ala}_{II}$ at 25° with magnesium ions at pH 7.5 (0.001 M Tris·HCl). pMg = $-\log [Mg^{2+}]$; Mg/P ratio = ratio of Mg^{2+} to tRNA organic phosphate. The arrows on the Mg/P scale indicate the point at which Mg/P = 0.5.

Mg^{2+} is added (Penniston and Doty, 1963a). This change is accompanied by a marked decrease in the number of residues that react with formaldehyde (Penniston and Doty, 1963b), a decrease in the exchange rate of slowly exchanging tritium (Englander and Englander, 1965), and a decrease in the rate of nuclease digestion of tRNA (Nishimura and Novelli, 1963, 1964). However, the precise nature of the conformational change that is induced by Mg^{2+} is not clearly understood.

Previous studies on this phenomenon have utilized either unfractionated or partially purified tRNA. The best samples, though specific for a single amino acid, contained variable quantities of isoaccepting or denatured material whose properties may differ substantially from those of native tRNA (Fresco *et al.*, 1966; Adams *et al.*, 1967). Clearly, it is desirable to work with pure samples of individual tRNA species. This avoids possible masking of conformational changes by sample heterogeneity and makes it possible to compare the properties of tRNAs having different sequences. One of the alanine tRNAs, $tRNA^{Ala}_{II}$, fulfills this requirement. It is homogeneous as judged by its oligonucleotide pattern obtained by digestion with RNase T-1 (Reeves *et al.*, 1968) and it is 97% pure based on a theoretical specific activity of 0.0128 pmole of alanine esterified/pmole of tRNA-phosphate (see Experimental Section). The other preparation, though free of other tRNAs and denatured material, is still a mixture of about two-thirds $tRNA^{Ala}_{Ia}$ and one-third $tRNA^{Ala}_{Ib}$. The substitution of a dihydroU for a U residue that distinguishes $tRNA^{Ala}_{Ia}$ from $tRNA^{Ala}_{Ib}$ is not expected to alter the Mg^{2+} effect very much. Therefore, it seems valid to compare this effect in $tRNA^{Ala}_{Iab}$ with that of $tRNA^{Ala}_{II}$ by measuring changes in their ultraviolet absorption or circular dichroism spectra in the presence and absence of Mg^{2+}.

Ultraviolet Absorption. The optical properties of highly purified yeast $tRNA^{Ala}_{Iab}$ and $tRNA^{Ala}_{II}$ are strongly dependent on magnesium ion concentration. The change in absorbance as a function of $-\log [Mg^{2+}]$ is shown in Figure 1. A sharp hypochromic effect is observed both at 260 nm and 280 nm at Mg^{2+} concentrations between 10^{-5} and 10^{-4} M. The change is complete when the Mg^{2+} to nucleotide phosphate ratio is 0.5. The narrow breadth of the transition and the lack of any magnesium dependence outside the transition region suggest that a cooperative transformation between two distinct structural types has occurred.

Although the Mg^{2+} effect is qualitatively similar in both tRNAs, the magnitude of the change at both wavelengths is greater for $tRNA^{Ala}_{II}$ than for $tRNA^{Ala}_{Iab}$. This might reflect a difference in the nucleotide composition of the regions of these two tRNAs that are undergoing a change in conformation, or it might mean that a greater number of base pairs are involved in the conformational change of $tRNA^{Ala}_{II}$ than in $tRNA^{Ala}_{Iab}$. Other results (see below) support the first conclusion.

Circular Dichroism. In order to gain further insight into the nature of the conformational change brought about by Mg^{2+}, we have investigated the effect of Mg^{2+} on the circular dichroism spectra of $tRNA^{Ala}_{Iab}$ and $tRNA^{Ala}_{II}$. The results are shown in Figure 2 and Table I. In the absence of Mg^{2+} both spectra show negative bands at 233–234 nm and strong, positive bands at 266–267. When Mg^{2+} is added, the 266–267 nm band shifts 6 nm toward the blue and increases in intensity. At the same time, a new negative band appears at 293 nm. Above 10^{-4} M, Mg^{2+} has no further

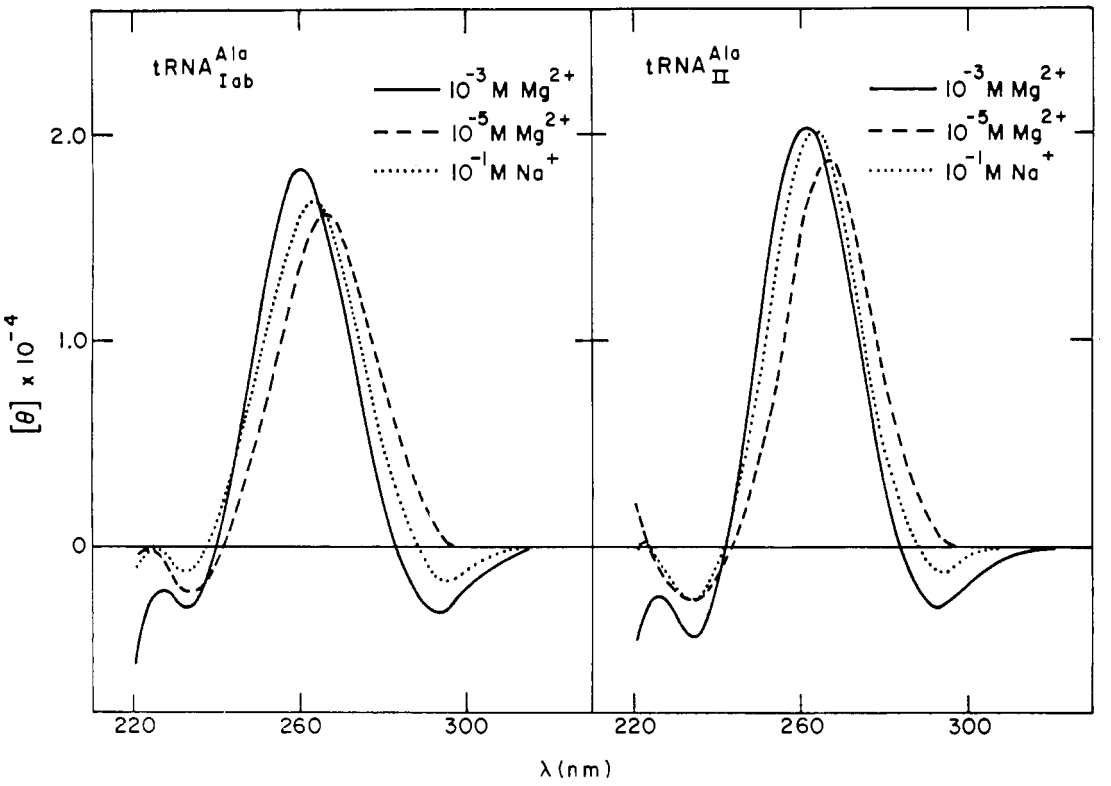

FIGURE 2: Circular dichroism spectra at 26° of $tRNA^{Ala}_{Iab}$ and $tRNA^{Ala}_{II}$ at pH 7.5 (0.001 M Tris·HCl) and the ionic conditions specified in the figure.

TABLE I

	Molar Extinction Coefficients		Circular Dichroism Spectra				Melting Curves
$tRNA^{Ala}_{Iab}$	$\epsilon_{260} \times 10^{-5}$	$\epsilon_{280} \times 10^{-5}$	λ_{max} (nm)	$\theta_{max} \times 10^{-3}$	λ_{min} (nm)	$\theta_{min} \times 10^{-3}$	T_m
$<10^{-6}$ M Mg^{2+}	6.15	3.20	266	16.7			55
$>10^{-3}$ M Mg^{2+}	5.56	2.70	260	18.2	293	−3.23	83
$tRNA^{Ala}_{II}$							
$<10^{-6}$ M Mg^{2+}	6.60	3.40	267	18.6			52
$>10^{-3}$ M Mg^{2+}	5.62	2.75	261	20.2	293	−2.96	74

effect, as expected from the titration curves (Figure 1). It must be emphasized that these changes are not Mg^{2+} specific. Similar changes are produced by Na^{+}, but Mg^{2+} is between 1000 and 10,000 times more effective in producing the conformational change. It should also be noted that the negative 293 nm band provides a sensitive test for the presence of Mg^{2+} in samples of $tRNA^{Ala}$ at low ionic strength.

From the results shown in Figure 2 and Table I, it is clear that the positive circular dichroism band is slightly more intense in $tRNA^{Ala}_{II}$ than in $tRNA^{Ala}_{Iab}$. This difference amounts to about 2×10^3 degrees ellipticity in the presence of Mg^{2+}, and 1.9×10^3 degrees ellipticity in the absence of Mg^{2+}. The weak, negative band at 293 nm is of particular interest. It was first observed in unfractionated tRNA by Sarker *et al.* (1967). It has never been found in single strand oligonucleotides or polynucleotides. It is present, however, in many, though not all, nucleic acids having appreciable double stranded regions. The intensity of this band varies greatly and is considerably greater in yeast $tRNA^{Ala}$ than in certain other tRNAs such as yeast $tRNA^{Phe}$ (K. Beardsley and C. R. Cantor, unpublished).

Interpretation of Circular Dichroism Spectra. Two aspects of the circular dichroism data shown in Figure 2 require an explanation. These are the greater overall intensity of the bands in $tRNA^{Ala}_{II}$ and the blue shift of the main band with appearance of the 295 nm band which accompanies the addition of magnesium ion. Both of these observations can be rationalized by the use of semiempirical, nearest-neighbor calculations (Cantor and Tinoco, 1965; Cantor *et al.*, 1966). These calculations were originally developed for the analysis

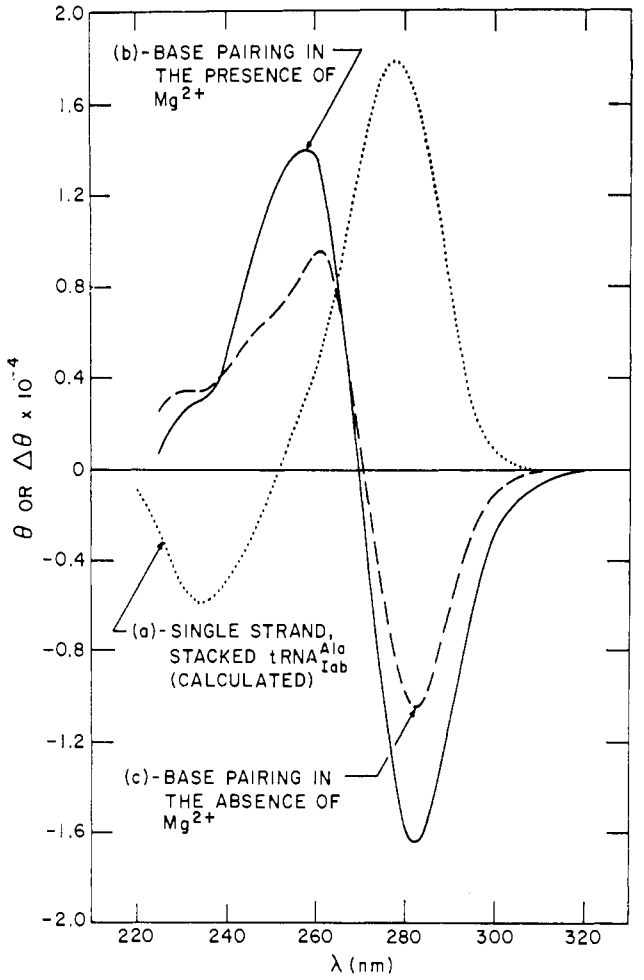

FIGURE 3: Calculated curves representing the contributions of base stacking and base pairing to the circular dichroism spectrum of $tRNA^{Ala}_{Iab}$. For the spectrum (curve a) for single strand, stacked $tRNA^{Ala}_{Iab}$, θ was calculated by the nearest-neighbor method (see text). For the difference spectrum (curve b) representing the contribution of base pairing to the most ordered structure of $tRNA^{Ala}_{Iab}$, $\Delta\theta$ was calculated by subtracting curve a from the experimental spectrum of $tRNA^{Ala}_{Iab}$ measured in the presence of Mg^{2+} (Figure 2). For the difference spectrum (curve C) representing the contribution of base pairing to the structure of $tRNA^{Ala}_{Iab}$ in the absence of Mg^{2+}, $\Delta\theta$ was calculated by subtracting curve a from the experimental spectrum of $tRNA^{Ala}_{Iab}$ measured in the absence of Mg^{2+} (Figure 2).

of optical rotatory dispersion, but they are equally valid for circular dichroism data (Cantor *et al.*, 1970).

The nearest-neighbor method requires a library of spectral data on oligonucleotides or polynucleotides in known conformations in order to calculate the circular dichroism of other oligo- or polynucleotides as a function of their structure. At present, unstacked and base-stacked conformations can be accounted for fairly precisely because of the complete library of mono- and dinucleoside phosphate circular dichroism data that has been accumulated (Warshaw and Cantor, 1970). The circular dichroism of double strand conformations and any anomalous optical activity expected at loops or hairpins cannot, as yet, be predicted with great accuracy owing to the lack of a suitably large set of reference compounds.

Using the nearest-neighbor approach, we first calculated the circular dichroism of yeast $tRNA^{Ala}_{Iab}$ as it would appear if the RNA were a single strand, stacked helix. This result is shown in Figure 3, curve a. It is subject to the same approximations and limitations used in earlier optical rotatory dispersion calculations (Cantor *et al.*, 1966; Vournakis and Scheraga, 1960). There is no 295 nm negative band and the peak of the positive band appears at 278 nm. This is located 12 nm to the red of the observed peak (Figure 2) at low Mg^{2+} concentration and 18 nm to the red of the peak observed at high concentrations of Mg^{2+}.

The calculated curve for $tRNA^{Ala}_{Iab}$ (Figure 3, curve a) is clearly in poor agreement with the experimental results (Figure 2), suggesting that a single strand stack is a poor representation of the conformation of tRNA both in the presence and absence of Mg^{2+}. It is not yet possible to perform a similar calculation for $tRNA^{Ala}_{II}$ since the sequence of this molecule is not yet completely known. However, comparison of the base composition and oligonucleotide fragment analysis of the two alanine tRNAs indicates that $tRNA^{Ala}_{II}$ contains several more adenosine residues than $tRNA^{Ala}_{Iab}$ (Holley *et al.*, 1965; Merrill, 1968; Reeves *et al.*, 1968). The circular dichroism of single strand oligonucleotides containing at least one adenosine is almost always more intense than the circular dichroism of other oligomers (Warshaw and Cantor, 1970). Rough estimates of the circular dichroism of $tRNA^{Ala}_{II}$ suggest that the difference in base composition alone is probably sufficient to account for the overall difference in the observed circular dichroism of the two polymers.

To further analyze the circular dichroism curves shown in Figure 2, we could attempt to match these experimental results with a linear combination of calculated single- and double-strand circular dichroism spectra. This approach, which has been used several times in the past year (Cantor *et al.*, 1966; Cantor, 1968), is capable in principle of yielding a good estimate for the extent of double strand helix in the tRNA molecule. Unfortunately, the circular dichroism library of double strand ribopolymers with regularly alternating sequence is not very complete at the present time. Prior calculations made use of this relatively small library, but recent studies on the circular dichroism of double strand DNAs of alternating sequence have shown that there is substantial sequence dependence of the optical properties of these compounds (B. E. Shortle, R. D. Wells, and C. R. Cantor, unpublished results). Thus, the estimates of double strandedness might be subject to significant errors. To circumvent this problem, we have developed an alternative approach. This uses the calculated single strand circular dichroism (Figure 3, curve a) as a base line which is subtracted from experimentally observed data (Figure 2). The difference circular dichroism spectrum which results should be proportional to contributions from double strand regions plus the effects of loops or hairpins, if any. Two such difference circular dichroism spectra for $tRNA^{Ala}_{Iab}$ are shown in Figure 3, curves b and c. The important features are summarized in Table II.

The circular dichroism difference spectrum of yeast $tRNA^{Ala}_{Iab}$ in the presence of Mg^{2+} (curve b) is very similar in shape to the difference spectrum in the absence of Mg^{2+} (curve c). Both show a negative band centered at 282.5 nm and a positive band at 258–260 nm. To generate a library

TABLE II: Circular Dichroism Difference Curves.

	Extrema and Crossovers Are Shown				
	$\Delta\theta_1$ ($\times 10^{-4}$)	λ_1 (nm)	λ_0 (nm)	$\Delta\theta_2$ ($\times 10^{-4}$)	λ_2 (nm)
$tRNA^{Ala}_{Iab}$ [high Mg^{2+} − low Mg^{2+}][a]	−0.57	282.5	266	+0.59	255
$tRNA^{Ala}_{Iab}$ [high Mg^{2+} − single strand]	−1.64	282.5	269.5	+1.40	257.5
$tRNA^{Ala}_{Iab}$ [low Mg^{2+} − single strand]	−1.01	282.5	270.5	+0.95	259
$tRNA^{Ala}_{II}$ [high Mg^{2+} − low Mg^{2+}]	−0.53	282.5	267	+0.77	255

[a] High $Mg^{2+} = 10^{-3}$ M; low $Mg^{2+} < 10^{-5}$ M.

of difference spectra, calculated single strand circular dichroism spectra were subtracted from measured circular dichroism of synthetic double strand polynucleotides. The difference spectra of virtually all compounds in this library are very similar to those obtained for tRNA (B. E. Shortle and C. R. Cantor, unpublished results). The difference circular dichroism spectra of the model polynucleotide, double helices must surely arise from the formation of base pairs. Thus, we feel justified in using the magnitude of the $tRNA^{Ala}_{Iab}$ difference spectrum as a measure of extent of base pairing. From the magnitude of the circular dichroism difference curves shown in Figure 3, one can easily conclude that, even in the absence of Mg^{2+}, $tRNA^{Ala}_{Iab}$ still contains a significant amount of double stranded structure and that the number of base pairs increases by about one-third when Mg^{2+} is added.

The origin of the 293 nm negative band is also suggested from the curves in Figure 3. Notice that the band at 282.5 nm in the difference spectrum (curve b or c) is strongly negative. This suggests that the small negative band seen in the experimental spectra (Figure 2) is a resultant of the relative magnitudes of the positive circular dichroism band due to base stacking (Figure 3, curve a) and the negative component of the double Cotton effect produced by base pairing (Figure 3, curve b or c).

A difference spectrum analysis of this kind is not possible with $tRNA^{Ala}_{II}$ because the sequence required for calculation of the single strand spectrum is not known. We approached this problem as follows. First we generated another difference curve that specifically represents the effect of Mg^{2+} on the conformation of $tRNA^{Ala}_{Iab}$ by subtracting the observed circular dichroism spectrum in the absence of Mg^{2+} from that obtained in the presence of Mg^{2+} using the data in Figure 2. A similar curve was calculated for $tRNA^{Ala}_{II}$ from the data in Figure 2. These difference spectra are shown in Figure 4 and the important features are summarized in Table II, lines 1 and 4.

The Mg^{2+}-induced difference spectra of the two tRNAs are very similar. This indicates that the conformational change brought about by magnesium removal must be just about the same in the two tRNAs. The shape of the two circular dichroism difference curves in Figure 4 is extremely similar to the circular dichroism difference curves presented in Figure 3, curves b and c. This means that the circular dichroism change due to Mg^{2+} probably represents a change in the extent of base pairing in both $tRNA^{Ala}_{Iab}$ and $tRNA^{Ala}_{II}$. The magnitude of this change can be estimated by comparing the two sets of difference curves. An examination of the data shown in Table II indicates that about one-third of the base pairs are broken when Mg^{2+} is removed from an alanine tRNA. For $tRNA^{Ala}_{Iab}$ the actual estimates are 38% if the 282.5 nm band is used (compare $\Delta\theta_1$ in lines 2 and 3 of Table II) and 32% if the shorter wavelength difference band is used (compare $\Delta\theta_2$ in lines 2 and 3 of Table II). This result is in good agreement with estimates based on ultraviolet hyperchromicity (see next section).

Melting Curves. As just pointed out, the conformational change induced by Mg^{2+} represents only a fraction of the total ordered structure. This is also shown in Figure 5. The hyperchromic effect at 25° represents the Mg^{2+}-induced conformational change while the total hyperchromic effect

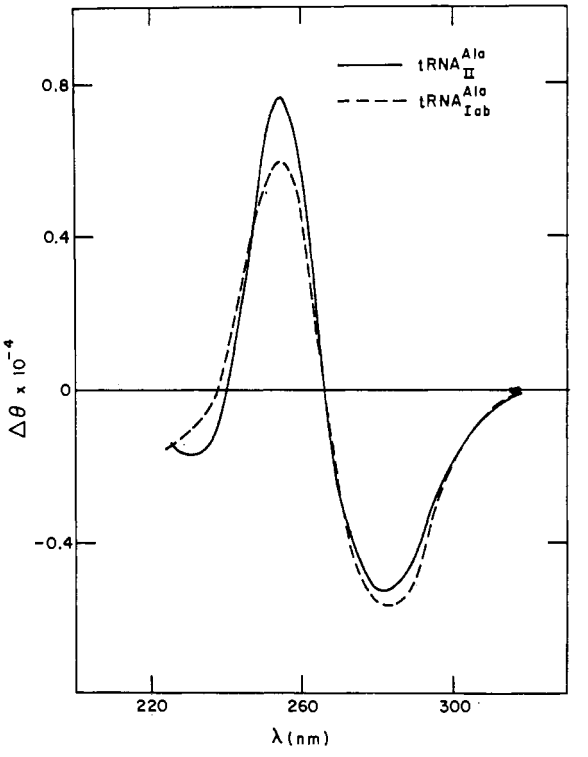

FIGURE 4: Circular dichroism difference spectra for $tRNA^{Ala}_{Iab}$ and $tRNA^{Ala}_{II}$ at pH 7.5 (0.001 M Tris·HCl) in the presence and absence of magnesium. These curves were obtained by point by point subtraction of the data in Figure 2.

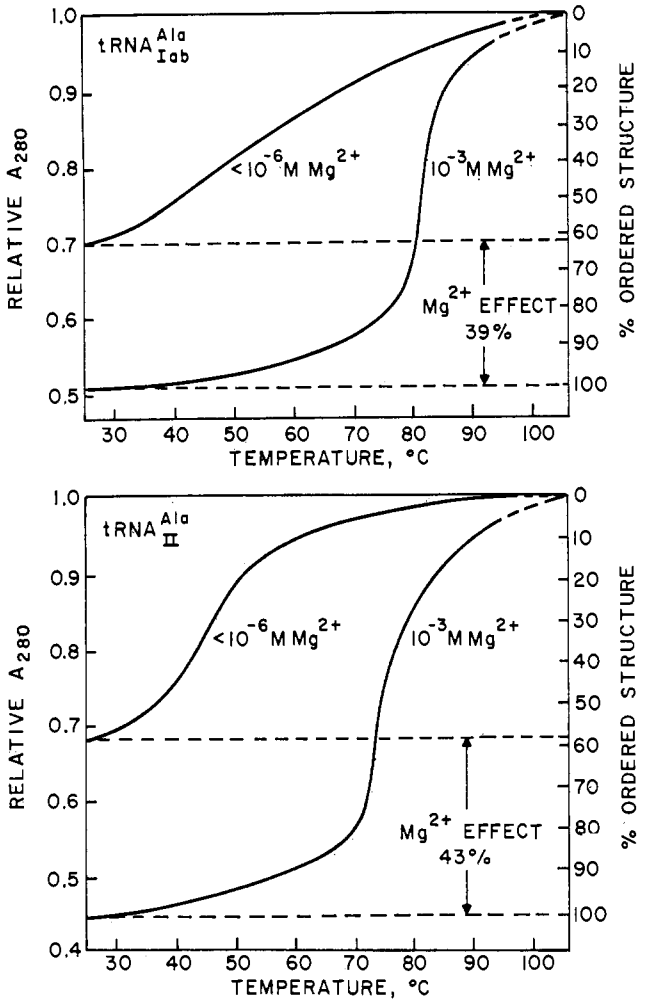

FIGURE 5: Melting curves of $tRNA^{Ala}_{Iab}$ and $tRNA^{Ala}_{II}$ at pH 7.5 (0.001 M Tris·HCl) in the presence and absence of magnesium ions.

observed in the presence of Mg^{2+} represents the complete disruption of ordered structure.

Quantitative measurements of the total hyperchromic effect are complicated by several factors. First, in the presence of Mg^{2+} melting is not complete at 95° (the highest temperature measured), and it is necessary to extrapolate the curve to obtain the relative A_{280} of the completely melted structure. Secondly, the relative A_{280} at 95° increases with increasing Mg^{2+} concentrations (data not shown). This is due, at least in part, to hydrolysis of the tRNA at high temperatures in the presence of Mg^{2+} since examination of the tRNA by gel filtration on Sephadex G-100 after cooling it back to room temperature showed the presence of oligonucleotide fragments (L. H. Schulman and R. W. Chambers, unpublished). These factors complicate the selection of data for calculating the fraction of the total structure represented by the Mg^{2+} effect. We have assumed that there is no difference between the melted structures obtained in the presence and absence of Mg^{2+}, *i.e.*, the melting curves fuse when melting is complete under both conditions. If this is true, then the curve measured in the absence of Mg^{2+} can be used to estimate the top of the hyperchromic effect. This

TABLE III:[a] Acceptor Activity When $tRNA^{Ala}$ Is Preincubated at the Temperature and [Mg^{2+}] Indicated for 3 min before Addition of a Reaction Mixture Containing Alanine, ATP, $MgCl_2$, Buffer, and Enzyme (see Experimental Section). Assays Were Conducted at the Same Temperature as the Preincubation.

tRNA	[Mg^{2+}] M	Spec Act. 25°	% Theory	Spec Act. 5°	% Theory
Ala Iab	$<10^{-6}$	1000	61[a]	180	11[a]
	10^{-5}	1090	66[a]	150	9[a]
	10^{-4}	1520	88[b]	1400	79[b]
	10^{-3}	1600	93[b]	1580	89[b]
	10^{-2}	1600	93[b]	1500	84[b]
Ala II	$<10^{-6}$	1560	103[c]	1580	104[c]
	10^{-5}	1750[e]	109[c]	1620	101[c]
	10^{-4}	1660	93[d]	1710	96[d]
	10^{-3}	1770	99[d]	1700	96[d]
	10^{-2}	1710	96[d]	1630	92[d]

[a] Theory = 1630 pmoles/A_{260}. [b] Theory = 1780 pmoles/A_{260}. [c] Theory = 1520 pmoles/A_{260}. [d] Theory = 1780 pmoles/A_{260}. [e] This value is probably in error. It is very difficult to determine the specific activity from absorbance measurements in this concentration of Mg^{2+} because of hyperchromicity charges (see Figure 1).

procedure avoids the problem of hydrolysis catalyzed by Mg^{2+} and provides the most reliable extrapolation.

Interpretation of the hyperchromic changes occurring upon heating the tRNA solution is complicated by the fact that the increased absorbance can arise both from unpairing of bases and from unstacking of nonpaired, stacked regions. Boedtker (1967) has shown that the hyperchromicity arising from unstacking of bases in formaldehyde-treated, unfractionated, yeast tRNA is quite small (less than 10%). Therefore, in agreement with our conclusions from circular dichroism data, the changes in ordered structure reflected in the melting curves, both in the presence and absence of Mg^{2+}, are due mainly to the disruption of base pairs. The magnitude of the Mg^{2+} effect seen in Figure 5 (39% for $tRNA^{Ala}_{Iab}$ and 43% for $tRNA^{Ala}_{II}$) is quite close to that estimated from circular dichroism data (32–38% for $tRNA^{Ala}_{Iab}$) even without attempting to correct the melting data for possible contributions of unstacking. Thus, both circular dichroism and melting curves indicate that removal of magnesium from either $tRNA^{Ala}_{Iab}$ or $tRNA^{Ala}_{II}$ results in the loss of about one-third of the total base pairs present in the most ordered structures; approximately two-thirds of the base paired regions remain intact even in the absence of Mg^{2+}.

The melting profiles provide additional evidence that Mg^{2+} induces similar conformational changes in both tRNAs, yet simple inspection of the data in Figure 5 and Table I shows clear differences between them. Once again, these differences probably reflect differences in base composition of the two tRNAs. The greater T_m of $tTNA^{Ala}_{Iab}$ compared

with $tRNA_{II}^{Ala}$, for example, probably reflects a higher GC pairing in agreement with the other optical data.

Aminoacyl Acceptor Activity. The effect of these conformational changes on biological activity is of considerable interest. In a footnote, Lindahl *et al.* (1967) stated that $tRNA^{Ala}$ can be trapped in a denatured (inactive) conformation at 0° in the absence of Mg^{2+}, but renaturation occurs rapidly in the presence of Mg^{2+} at 25°. We have confirmed and extended this observation.

Solutions of $tRNA_{Iab}^{Ala}$ containing various amounts of Mg^{2+} were preincubated for 3 min at either 25 or 5°. The components of the assay mixture, including Mg^{2+} (20 mM), were then added and the assay was conducted at the same temperature as the preincubation. The results are shown in Table III.

When a Mg^{2+}-free solution of $tRNA_{Iab}^{Ala}$ is cooled to 5° prior to addition of Mg^{2+}, it has very little biological activity (specific activity 180). The low activity is not due to a slow rate of aminoacylation because addition of Mg^{2+} (10^{-3} M) prior to cooling gives a high activity (1580 pmoles/A_{260}). This indicates that the Mg^{2+}-free conformation of $tRNA_{Iab}^{Ala}$ is inactive. At 5°, it is trapped in this denatured state by addition of Mg^{2+} at the time of assay (specific activity 180). If the Mg^{2+} is added at 25°, however, then considerable activity (specific activity 1000) is observed.

Comparison of the activities after adjusting the solution to various concentrations of Mg^{2+} at 25° followed by the assay at either 25 or 5° shows a sharp increase in activity between 10^{-5} and 10^{-4} M (Table III). This parallels the conformational changes induced by Mg^{2+} (Figure 1). Once this change has occurred, however, the activities are almost the same regardless of the assay temperature.[4]

Similar experiments with $tRNA_{II}^{Ala}$ gave very different results. As shown in Table III, the activities were essentially the same at both 5 and 25°. The small increase in apparent activity with increasing Mg^{2+} concentration may be due to the hyperchromic effect of Mg^{2+} (specific activity is expressed as pmoles of alanine loaded/A_{260}, and addition of Mg^{2+} causes the A_{260} to decrease). Thus, it was not possible to demonstrate any significant amount of denatured $tRNA_{II}^{Ala}$. This, of course, does not mean that inactive conformations of $tRNA_{II}^{Ala}$ do not exist, but only that it is not possible to trap them in a metastable state.

Discussion

Nature of the Conformational Change Induced by Mg^{2+}. The Mg^{2+} transition is cooperative and occurs when $Mg^{2+}/P = 0.5$. This suggests that all the tRNA phosphate residues must bind Mg^{2+} before the change can occur. Secondly, the melting curves (Figure 5) and the circular dichroism data presented in Figure 3 show quite clearly that the conformations existing in the absence of Mg^{2+} have considerable ordered structure (60% of the maximum).

These structural features seem to be general for all tRNAs. Penniston and Doty (1963a) found that unfractionated tRNA displayed considerable ordered structure at 25° in the absence of Mg^{2+}. They also found that addition of Mg^{2+} caused a pronounced, cooperative hypochromic effect when $Mg^{2+}/P = 0.5$. Their curve was broader than ours, of course, because they were measuring the average properties of an unfractionated mixture.

Both the circular dichroism spectra and the melting curves indicate that in the absence of Mg^{2+}, $tRNA_{Iab}^{Ala}$ and $tRNA_{II}^{Ala}$ still have ordered structures which contain about 66% of the base pairs present in the native structure. Since we do not know how many base pairs are present in the most ordered structures, it is impossible to calculate the actual number of new base pairs involved in the Mg^{2+}-induced, conformational change. Certainly, the use of the cloverleaf model as a measure of the total base pairs is not justified, since there is ample evidence from nuclease activity (Penswick, 1966; Armstrong *et al*, 1964) and chemical modification (Yoshida and Ukita, 1965, 1966; Bronstoff and Ingram, 1967; Nelson *et al.*, 1967) that an open cloverleaf is not an adequate description of $tRNA^{Ala}$ in solutions containing Mg^{2+}.

Apparently an open cloverleaf is not an adequate description of tRNA in the absence of Mg^{2+} either. Small angle X-ray scattering data from samples of purified $tRNA_{Iab}^{Ala}$ in the absence of Mg^{2+} can be fit to a model ellipsoid possessing an axial ratio of 4 (Krigbaum and Godwin, 1968). Krigbaum and Godwin point out that this axial ratio is inconsistent with the open cloverleaf model. Recent micrographs from dark field electron microscopy apparently show tRNA molecules in the cloverleaf structure (Ottensmeyer, 1969). This supports the idea that tRNA *can* assume a cloverleaf conformation and that this probably represents the "correct" secondary structure with native tRNA. However, *in solution* and in the absence of Mg^{2+}, $tRNA_{Iab}^{Ala}$ seems to be best represented by an elongated, partially base-paired model.[5]

Although no small angle X-ray data are available for $tRNA_{II}^{Ala}$, the molecular volumes of both the alanine tRNAs, as measured by gel filtration on Sephadex G-100, are similar (Imura *et al.*, 1969a; L. H. Schulman and R. W. Chambers, unpublished). In the absence of Mg^{2+}, both have retention constants (V_0/V_e) of 0.68. It seems likely, then, that $tRNA_{II}^{Ala}$ is also an elongated, partially base-paired molecule in the absence of Mg^{2+}. In the presence of Mg^{2+}, on the other hand, the retention constant for both alanine tRNAs on Sephadex G-100 is 0.58. Comparison of this value with that obtained in the absence of Mg^{2+} (0.68) indicates that both these tRNAs have a much more compact conformation in the presence of Mg^{2+} than in its absence. Ultracentrifugation studies (H. Warner, L. H. Schulman, and R. W. Chambers, unpublished) support this conclusion since the $s_{20,w}$ is higher (4.08) in the presence of Mg^{2+} than in its absence (3.74).

Our data (gel filtration, ultracentrifugation, and changes in optical properties) show that Mg^{2+} causes both $tRNA_{Iab}^{Ala}$ and $tRNA_{II}^{Ala}$ to fold into compact, ordered structures and that the folding process involves an increase in base pairs rather than just an increase in base stacking. Whether this change involves both secondary and tertiary structures or only one of them is speculative, but a further discussion

[4] Recent results indicate that 80% renaturation of $tRNA_{Iab}^{Ala}$ can be achieved by warming the Mg^{2+}-containing solution to 37° prior to assay at any temperature down to 5° (G. B. Weiss and R. W. Chambers, unpublished data).

[5] Molecular weight determinations (unpublished data) indicate that $tRNA^{Ala}$ is monomeric under the conditions we have employed. However, dimers have been demonstrated (Loehr and Keller, 1968).

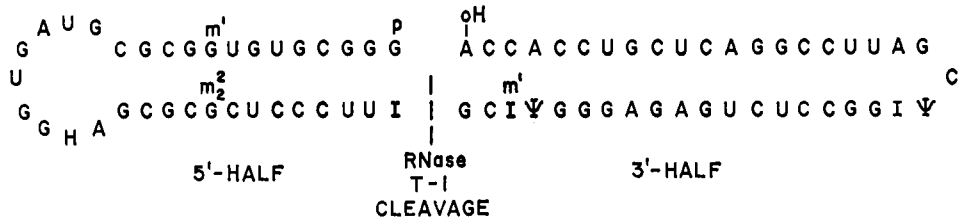

FIGURE 6: Possible ordered structures formed from "half" molecules of $tRNA^{Ala}_{Iab}$ after cleavage at the anticodon with RNAse T-1.

of this in connection with denaturation will be found in the next section.

Denaturation. The different denaturation behavior of $tRNA^{Ala}_{Iab}$ and $tRNA^{Ala}_{II}$ and the relationship of this behavior to the Mg^{2+}-induced conformational change are particularly interesting. There is now good evidence that a correctly base-paired acceptor stem of the cloverleaf model is required for alanine acceptor activity (Schulman and Chambers, 1968; Imura *et al.*, 1969b; Chambers, 1969). It is tempting to equate opening and closing of the acceptor stem with the conformational change induced by Mg^{2+} since formation of the seven base pairs in this region seems about right for the optical changes that occur on addition of Mg^{2+}. Unfortunately, this simple explanation does not account for the different denaturation behavior of these two tRNAs.

It seems more likely that denaturation of $tRNA^{Ala}_{Iab}$ is due to folding of some secondary structure other than the cloverleaf with consequent interaction between segments of the molecule that leads to a "wrong" tertiary structure as suggested first by Fresco and his coworkers (Adams *et al.*, 1967). For example, the conformation of $tRNA^{Ala}_{Iab}$ in the absence of Mg^{2+} might be represented by an elongated, base paired model[6] as shown in Figure 6. We suggest that, in order to form an active molecule, rearrangement to form the cloverleaf with its correctly ordered acceptor stem must occur. In the absence of Mg^{2+}, the cloverleaf structure is in equilibrium with other secondary structures such as the one shown in Figure 6 and the relative stability of these structures will determine their proportions at a given temperature.

Our data show that the tRNA folds when Mg^{2+} is added. We suggest that "incorrect" structures which are relatively stable (*e.g.*, $tRNA^{Ala}_{Iab}$ at 5° as represented in Figure 6) fold without rearrangement to give a denatured tRNA. Less stable secondary structures (*e.g.*, $tRNA^{Ala}_{II}$) rearrange to the cloverleaf before folding to give native tRNA. This places the cloverleaf structure as a mandatory, though transitory, intermediate in the formation of native tRNA.

It should be made clear that the conformations of $tRNA^{Ala}_{Iab}$ and $tRNA^{Ala}_{II}$ that we have observed in the absence of Mg^{2+} do not represent the denatured form described by Fresco and his collaborators (Lindahl *et al.*, 1967). The conformation existing in the absence of Mg^{2+} has considerably less base pairing than denatured forms, which can only be demonstrated in the presence of Mg^{2+}. Our low Mg^{2+} tRNA probably corresponds closely to the transition state that denatured tRNA must pass through during the process of re-forming a cloverleaf secondary structure prior to folding into the renatured state.

We wish to emphasize that a unique tertiary structure of the entire molecule is not required for acceptor activity. Both changes in physical properties in *fully active* $tRNA^{Ala}_{Iab}$ after photochemical modification (Schulman and Chambers, 1968, 1970) as well as reconstitution of alanine acceptor activity from small fragments of $tRNA^{Ala}_{II}$ (Imura *et al.*, 1969a; Chambers, 1969) are inconsistent with this idea. All that seems to be required is that the acceptor stem be correctly ordered and that any additional ordered structure that is present does not interfere sterically with the elements of the acceptor stem that are required for recognition. Tertiary structure does not appear to be *required* for acceptor activity, but it seems to stabilize the acceptor stem region that is required for activity (Chambers, 1969).

Experimental Section

Sample Preparation. Samples of the two alanine tRNAs were prepared by the BD-cellulose method (Reeves *et al.*, 1968). Pools of the tRNAs (about 50 A_{260} units each) were examined for homogeneity as described previously. Neither was contaminated by the other. Magnesium ions were removed from each sample by dialysis against four 100-ml volumes (4 hr each) of 0.01 M sodium EDTA followed by three 100-ml volumes of glass distilled water. The ultraviolet spectra of these samples displayed end absorption starting at about 260 nm that indicated traces of EDTA remained in the sample. This was removed by passing 1-ml samples of the tRNA through a 1 × 30 cm Sephadex G-25 column that had been equilibrated with 0.001 M Tris·HCl, pH 7.5, at room temperature. Fractions were collected and examined by ultraviolet spectroscopy for EDTA. Those tRNA fractions found to be free of EDTA were used for the experiments described here. The specific activities in terms of alanine esterified were 1780 pmole/$A_{260}^{Mg^{2+}}$; $A_{260}^{Mg^{2+}}$ = absorbance measured in a 1-cm cell in the presence of 0.01 M $MgCl_2$ + 0.001 M Tris·HCl buffer, pH 7.5.

Sample Purity. Aliquots containing 1.0 A_{260} units of tRNA in 0.01 M $MgCl_2$ + 0.001 M Tris·HCl buffer, pH 7.5, were digested with 70% $HClO_4$ (King, 1932) and then diluted to 5.0 ml with triple glass distilled water. Aliquots (1 ml) were analyzed for inorganic phosphate by the micromethod of Chen *et al.* (1956). Aliquots of the same tRNA solution

[6] This model is meant only to be a representation of a secondary structure other than the cloverleaf. It also fits our physical data in a general way, but we do not wish to imply that this particular representation is any better than a number of other possibilities. It is based, however, on observations made by Penswick (1966) who found that half-molecules of $tRNA^{Ala}_{Iab}$ produced by cleavage with RNase T-1 and separated by DEAE chromatography had a large amount of ordered structure. He was unable to reconstitute activity from these halves and he suggested that the stable, ordered structure of the fragments prevented them from recombining.

used for phosphate analysis were also assayed for alanine acceptor activity. Organic phosphate values were divided by the number of nucleotide residues to obtain the pmoles of tRNA present in the sample. The specific activity in terms of pmoles of Ala-tRNA/pmole of tRNA phosphate was calculated from the alanine acceptor activity and the organic phosphate analysis. The theoretical value for both tRNAs based on 78 nucleotides is 0.0128; found, $tRNA^{Ala}_{Iab}$, 0.0123 (96%); $tRNA^{Ala}_{II}$, 0.0124 (97%). The specific activities of these samples in pmoles of alanine esterified/$A_{260}^{Mg^{2+}}$ = 1780.

Samples of each tRNA (2 A_{260} units) were digested with RNase T-1 and fractionated on DEAE-cellulose as described before (Reeves *et al.*, 1968). No evidence of contamination of $tRNA^{Ala}_{II}$ by other tRNAs was found, but $tRNA^{Ala}_{Iab}$ was a mixture of two species (see peak 13ab, Penswick and Holley, 1965; Reeves *et al.*, 1968). It is estimated that the ratio of $tRNA^{Ala}_{Ia}$ to $tRNA^{Ala}_{Ib}$ is about 2:1 on the basis of these peak areas.

Magnesium Ion Titrations. Aliquots of standardized $MgCl_2$ solutions were added to 2.0-ml samples of tRNA in 0.001 M Tris·HCl, pH 7.5, in 1-cm quartz cuvets. The total organic phosphate concentration of the $tRNA^{Ala}_{Iab}$ sample was 2.34×10^{-4} M; for $tRNA^{Ala}_{II}$, 1.55×10^{-4} M. Five minutes after each addition of $MgCl_2$, the absorbancy of the solution was measured at 260 and 280 nm with a Cary Model 14 spectrophotometer. All measurements were made at 25° using a thermostated cell compartment. The plots of absorbance against $-\log [MgCl_2]$ were corrected for the volume changes due to each addition of $MgCl_2$ solutions.

Ultraviolet Absorption Spectra. Spectra were measured with a Cary Model 14 spectrophotometer at 25° as described above. The tRNA solutions ($tRNA^{Ala}_{Iab}$ 3.00×10^{-6} M; $tRNA^{Ala}_{II}$, 1.99×10^{-6} M) contained 0.001 M Tris·HCl buffer, pH 7.5. The molar extinction coefficients are given in Table I.

Circular Dichroism Spectra. Circular dichroism measurements at 26° were performed with a Model 6001 circular dichroism attachment to the Cary Model 60 spectropolarimeter. A 3-sec time constant and a slit program giving a 1-nm band pass were used for all measurements. Data reduction was handled as described previously (Cantor, 1968). The concentration of $tRNA^{Ala}_{Iab}$ was 1.86×10^{-6} M; $tRNA^{Ala}_{II}$, 2.24×10^{-6} M. The total organic phosphate of each was $tRNA^{Ala}_{Iab}$, 1.45×10^{-4} M; $tRNA^{Ala}_{II}$, 1.75×10^{-4} M. All solutions contained 0.001 M Tris·HCl buffer, pH 7.5. All measurements were made at 26° in a 1-cm cell.

Enzymatic Assays. Aminoacylation was measured as described previously (Reeves *et al.*, 1968).

Melting Curves. The absorbance of $tRNA^{Ala}$ at 280 nm as a function of temperature was measured with a Beckman DB spectrophotometer connected to a Honeywell Electronik 19 recorder. The temperature was controlled with a Beckman T_m analyzer. Heating was carried out at a rate of 1.4°/min. The ambient temperature was recorded by means of a thermistor in the sample cell. All tRNA solutions contained 0.001 M Tris·HCl buffer, pH 7.5. The A_{280} at the start was about 0.15 in each case. The absorbance was corrected for volume changes that occurred during heating.

References

Adams, A., Lindahl, T., and Fresco, J. R. (1967), *Proc. Nat. Acad. Sci. U. S. 57*, 1684.

Armstrong, A., Hogopian, H., Ingram, V. M., Sjoquist, I., and Sjoquist, J. (1964), *Biochemistry 3*, 1194.

Boedtker, M. (1967), *Biochemistry 6*, 2718.

Bronstoff, S. W., and Ingram, V. M. (1967), *Science 158*, 666.

Cantor, C. R. (1968), *Proc. Nat. Acad. Sci. U. S. 59*, 478.

Cantor, C. R., Jaskunas, S. R., and Tinoco, I., Jr. (1966), *J. Mol. Biol. 20*, 39.

Cantor, C. R., and Tinoco, I., Jr. (1965), *J. Mol. Biol. 13*, 65.

Cantor, C. R., Warshaw, M. M., and Shapiro, H. (1970), *Biopolymers*, in press.

Chambers, R. W. (1969), *J. Cell. Physiol. 74, Suppl. 1*, 179.

Chen, P. S., Jr., Toribara, T. Y., and Warner, H. (1956), *Anal. Chem. 28*, 1756.

Englander, S. W., and Englander, J. J. (1965), *Proc. Nat. Acad. Sci. U. S. 53*, 385.

Fresco, J. R., Adams, A., Ascione, R., Henley, D., and Lindahl, T. (1966), *Cold Spring Harbor Symp. Quant. Biol. 31*, 527.

Holley, R. W., Everett, G. A., Madison, J. T., and Zamir, A. (1965), *J. Biol. Chem. 240*, 2122.

Imura, N., Schwam, H., and Chambers, R. W. (1969a), *Proc. Nat. Acad. Sci. U. S. 62*, 1203.

Imura, N., Weiss, G. B., and Chambers, R. W. (1969b), *Nature 222*, 1147.

Imura, N., Weiss, G. B., and Chambers, R. W. (1969c), *Biochemistry 8*, 4776.

King, E. J. (1932), *Biochem. J. 26*, 292.

Krigbaum, W. R., and Godwin, R. W. (1968), *Macromolecules 1*, 375.

Lindahl, T., Adams, A., and Fresco, J. (1967), *J. Biol. Chem. 242*, 3129.

Loehr, J. S., and Keller, E. B. (1968), *Proc. Nat. Acad. Sci. U. S. 61*, 115.

Merrill, C. R. (1968), *Biopolymers 6*, 1727.

Nelson, J. A., Ristow, S. C., and Holley, R. W. (1967), *Biochim. Biophys. Acta 149*, 590.

Nishimura, S., and Novelli, G. D. (1963), *Biochem. Biophys. Res. Commun. 2*, 161.

Nishimura, S., and Novelli, G. D. (1964), *Biochim. Biophys. Acta 80*, 574.

Ottensmeyer, F. D. (1969), *Biophys. J. 9*, 1144.

Penniston, J. T., and Doty, P. (1963a), *Biopolymers 1*, 145.

Penniston, J. T., and Doty, P. (1963b), *Biopolymers 1*, 209.

Penswick, J. R. (1966), "Contributions to the Structure Determination of Alanine Transfer Ribonucleic Acid from *Saccharomyces cerevisiae*," Ph.D. Thesis, University Microfilms, Inc., Ann Arbor, Mich.

Penswick, J. R., and Holley, R. W. (1965), *Proc. Nat. Acad. Sci. U. S. 53*, 543.

Reeves, R. H., Imura, N., Schwam, H., Weiss, G. B., Schulman, L. H., and Chambers, R. W. (1968), *Proc. Nat. Acad. Sci. U. S. 60*, 1450.

Sarker, P. K., Wells, B., and Yang, J. T. (1967), *J. Mol. Biol. 25*, 563.

Schulman, L. H., and Chambers, R. W. (1968), *Proc. Nat. Acad. Sci. U. S. 61*, 308.

Schulman, L. H., and Chambers, R. W. (1970), Symposium on Protein Biosynthesis, Olozytn, Poland, in press.

Vournakis, J. N., and Scheraga, H. A. (1966), *Biochemistry 5*, 2997.

Warshaw, M. M., and Cantor, C. R. (1970), *Biopolymers*, in press.

Yoshida, M., and Ukita, T. (1965), *J. Biochem.*, *58*, 191.

Yoshida, M., and Ukita, T. (1966), *Biochim. Biophys. Acta* *123*, 214.

Molecular Weight and Subunit Structure of Yeast Enolase*

Kenneth G. Mann,† Francis J. Castellino,‡ and Paul A. Hargrave

ABSTRACT: The native and subunit molecular weights of yeast enolase have been reinvestigated by sedimentation equilibrium analysis, gel filtration in guanidinium chloride, and gel electrophoresis in sodium dodecyl sulfate. The values obtained in this work with three different and highly purified enolase preparations are 88,000 daltons for the native (dimeric) enzyme and 44,000 daltons for the subunits. These new values are considerably higher than the published ones (67,000 and 34,000 daltons) and it will be necessary to reevaluate the published molecular properties of yeast enolase.

A molecular weight of 67,000 daltons has been generally accepted for yeast enolase for the last 20 years. This value has been arrived at by a number of different methods: mercury analysis of the crystalline Hg–enzyme and sulfur analysis assuming 1 mole of Hg^{2+} and 8 moles of S per mole of enzyme (Warburg and Christian, 1941), quantitative amino-terminal analysis (Malmström *et al.*, 1959; Brewer *et al.*, 1970), light-scattering measurements (Bucher, 1947), sedimentation–diffusion, and sedimentation equilibrium measurements (Bergold, 1946; Brewer and Weber, 1968; Gawronski and Westhead, 1969), all giving molecular weight values in the range from 64,000 to 68,000 daltons. Early unsuccessful attempts to effect subunit dissociation together with the evidence from the chemical analyses led to the conclusion that the enzyme consisted of a single polypeptide chain of molecular weight 67,000 daltons. More recently, the existence of subunits was clearly demonstrated by the observed reduction in molecular weight to 34,000 daltons when the enzyme was exposed to high concentration of KCl or KBr in the absence of Mg^{2+} (Brewer and Weber, 1968; Gawronski and Westhead, 1969).

In our studies of the subunit structure and chemical properties of yeast enolase, we accumulated a number of quantitative data which were incompatible with a molecular weight of 67,000 daltons and consequently decided to reinvestigate the molecular weight of both the native enzyme and its subunits. The results of this investigation are reported here and lead to a revised molecular weight of 85,000–90,000 daltons for yeast enolase.

The existence of multiple molecular forms of yeast enolase has been well documented (Malmström, 1957; Westhead and McLain, 1964). It is, therefore, conceivable that variations in results from different laboratories and at different times are due to different sources of yeast or to differences in isolation procedures leading to the purification of different enolase isozymes. These possible variations were checked to a limited extent in this work by comparing three different preparations of yeast enolase, two obtained from separate batches of Fleischmann bakers yeast (Pekin, Ill.) at an interval of 6 months and one obtained from brewer's yeast (Carling Brewing Co., Atlanta, Ga.).[1] The purity and specific activity measurements and some of the molecular weight studies were carried out for these three enzymes in parallel experiments. The three preparations are identified as P, Q, and R.

Experimental Section

Activity Assay. Enolase activity was measured by the direct spectrophotometric assay of phosphoenolpyruvate production monitored at 230 nm at 30° (Westhead, 1966). The substrate, barium D-glycerate 2-phosphate (Sigma), was converted into and used as the water-soluble cyclohexylammonium salt.

Purification of Enzyme. Enolase was prepared according to the method described by Westhead (1966). The final product of each individual preparation was subjected to chromatography on TEAE-cellulose[2] (Westhead and McLain, 1964) to separate different active enolase species, and the subsequent work was done only with the so called A isozyme (the first major peak eluted from the TEAE-cellulose column). The purity of each, preparation was checked by specific activity measurements, disc gel electrophoresis, and isoelectric focusing.

Physical Methods. Polyacrylamide gel electrophoresis was

* From the Department of Biochemistry, Duke University Medical Center, Durham, North Carolina 27706, and the Department of Biochemistry, University of Minnesota, Minneapolis, Minnesota 55455. *Received May 29, 1970.* Supported in part by U. S. Public Health Service Research grants (AM-04576, HE-06400, and GM-15053), Postdoctoral Fellowships (GM-34119 (K. G. M.) and AM-34008 (F. J. C.)), and Predoctoral Fellowship (GM-33541 (P. A. H.)).

† Present address: Department of Biochemistry, University of Minnesota, St. Paul, Minn. 55101; to whom to address correspondence.

‡ Present address: Department of Chemistry, University of Notre Dame, Notre Dame, Ind. 46556.

[1] We are greatful to Dr. J. M. Brewer for providing us with this purified enolase and thus enabling us to carry out the comparative work.

[2] Abbreviations used are: TEAE, triethylaminoethyl; Gu·HCl, guanidinium chloride.